DP-MS-79-41



# Appraisal of Multidimensional Space-Time Kinetics Studies

W. G. Winn, N. P. Baumann, and C. E. Jewell

E. I. du Pont de Nemours and Company
Savannah River Laboratory
Aiken, South Carolina 29801



A paper submitted for publication in *Nuclear Science and Engineering* as a Technical Note. Please send proofs, etc. to N. P. Baumann.

Pages: 10

Tables: 4

Figures: 3

---

This document was prepared in conjunction with work accomplished under Contract No. DE-AC09-76SR00001 with the U.S. Department of Energy.

**DISCLAIMER**

# APPRAISAL OF MULTIDIMENSIONAL SPACE-TIME NUCLEAR KINETICS STUDIES*

W. G. Winn, N. P. Baumann, and C. E. Jewell

## ABSTRACT

Diffusion theory analysis of a series of multidimensional space-time experiments is appraised in terms of the final experiment of the series. In particular, TRIMHX diffusion calculations were examined for an experiment involving free-fall insertion of a $^{235}U$-bearing rod into a heavy-water-moderated reactor with a large reflector. The experimental, transient flux-tilts were accurately reproduced after cross section adjustments forced agreement between static diffusion calculations and static reactor measurements. The time-dependent features were particularly well-modeled, and the bulk of the small discrepancies in space-dependent features should be removable by more refined cross section adjustments. This experiment concludes a series of space-time experiments which span a wide range of delayed neutron holdback effects. TRIMHX calculations of these experiments demonstrate the accuracy of the time-dependent modeling employed in the code.

---

*Work performed under USDOE Contract No. AT(07-2)-1.

# I. INTRODUCTION

The TRIMHX code[1] performs diffusion calculations which agree well with 2-dimensional[2] and 3-dimensional[3] space-time experiments, provided that cross section parameters are adjusted to give agreement with similar static experiments. Each of these experiments used identical fuel loadings but different control rod configurations, so that TRIMHX could be tested for a variety of neutronic coupling strengths for the reactor. Changing the number of fuel elements in the reactor is also a means of varying the neutronic coupling strength. The present study tests TRIMHX for a reduced fuel loading that is surrounded by a large reflector.

This series of experiments was performed in the heavy-water-moderated Process Development Pile (PDP)[4] at the Savannah River Laboratory. As in the earlier studies,[2,3] the present work utilized a series of static reactor measurements to make appropriate cross section adjustments for the TRIMHX analysis. Then $^{235}U$ fuel was rapidly inserted near the core-reflector interface to initiate the transient experiment.

The resulting transient flux is tilted relative to the pre-transient static flux. A "tilt" at time t after initiating the transient is defined[2,3] as

$$\text{Tilt (A/B)} = \frac{[\phi(t)/\phi(o)]_A}{[\phi(t)/\phi(o)]_B} \qquad (1)$$

where $\phi(t)$ and $\phi(o)$ are fluxes at positions A and B. The predicted fluxes and tilts for several detector pairs are compared with experimental data, and discrepancies are appraised in terms of their space- and time-dependent deviations.

The present and earlier studies span a comprehensive set of reactor loadings for which TRIMHX has been tested. A reactor coupling strength for each loading is defined and correlated with the delayed neutron holdback (DNH)[5] exhibited during each transient. The time scale of the perturbation does not permit examination of fast neutronics effects such as kinetic distortion.[5]

## II. DISCUSSION

### A. General Considerations

In these studies, two time regions of the transient neutronic behavior were examined. Early in the transient, but after the prompt jump, DNH prevented immediate assumption of the asymptotic flux shape. Later in the transient, the flux increased exponentially with a space-independent period. The flux tilts readily displayed the DNH effects; the asympototic exponential flux provided data for measuring the insertion worth.

### B. DNH Time Region

A time-dependent flux tilt may be expressed as,

$$\text{Tilt (A/B)} = T(\vec{r},t) = 1 + f(\vec{r},t)[T(\vec{r},\infty) - 1] \qquad (2a)$$

where the detector specification (A/B) is functionally represented by the detector coordinates $(\vec{r}_A,\vec{r}_B) \equiv (\vec{r})$. The asymptotic tilt $T(\vec{r},\infty)$ has no time dependence but depends on the spatial coordinates of the detector pair. Thus, in principle, $T(\vec{r},\infty)$ is determined from static experiments alone; and agreement between TRIMHX and experimental values of $T(\vec{r},\infty)$ is directly influenced by the

cross section adjustments.[6] By contrast, the function $f(\vec{r},t)$ depends on DNH modeling and has the properties

$$f(\vec{r},t) = 0, \quad t \leq 0$$

$$f(\vec{r},t) = 1, \quad t \to \infty$$

Normally $f(\vec{r},t)$ is predominantly time-dependent, having only a weak space-dependence compared to $T(\vec{r},\infty)$.

TRIMHX tilts, $T_c(t)$, were compared with experimental tilts, $T_e(t)$. These can be expressed as

$$T_c(\vec{r},t) = 1 + f_c(\vec{r},t)[T_c\ \vec{r},\infty) - 1] \tag{2b}$$

$$T_e(\vec{r},t) = 1 + f_e(\vec{r},t)[T_e(\vec{r},\infty) - 1] \tag{2c}$$

The functional deviation $\delta T(\vec{r},t)$ between calculated and experimental tilts is conveniently expressed as

$$\begin{aligned} \delta T(\vec{r},t) &= T_c(\vec{r},t) - T_e(\vec{r},t) \\ &= [T_c(\vec{r},t) - T_d(\vec{r},t)] + [T_d(\vec{r},t) - T_e(r,t)] \\ &= \delta T_s(\vec{r},t) + \delta T_t(\vec{r},t), \end{aligned} \tag{3}$$

where $T_d(\vec{r},t)$ is selected so that $\delta T(\vec{r},t)$ is expressed as the sum of a predominantly space-dependent deviation $\delta T_s(\vec{r},t)$ and a predominantly time-dependent deviation $\delta T_t(\vec{r},t)$. Selecting $T_d(\vec{r},t)$ as

$$T_d(\vec{r},t) = 1 + f_c(\vec{r},t)[T_e(\vec{r},\infty) - 1] \tag{4}$$

yields

$$\delta T_s(\vec{r},t) = T_c(\vec{r},t) - T_d(\vec{r},t) = f_c(\vec{r},t)\ \delta T(\vec{r},\infty) \qquad (5a)$$

$$\delta T_t(\vec{r},t) = T_d(\vec{r},t) - T_e(\vec{r},t) = [T_e(\vec{r},\infty) - 1]\ \delta f(\vec{r},t) \qquad (5b)$$

where $\delta T(\vec{r},\infty) = T_c(\vec{r},\infty) - T_e(\vec{r},\infty)$ and $\delta f(\vec{r},t) = f_c(\vec{r},t) - f_e(\vec{r},t)$. The $\delta T(\vec{r},\infty)$ factor indicates that the functional deviation $\delta T_s(\vec{r},t)$ is primarily space-dependent. Similarly, $\delta T_t(\vec{r},t)$ is primarily time-dependent due to the $\delta f(\vec{r},t)$ factor.

The total deviation $\delta T(\vec{r},t)$ is examined in terms of $\delta T_s(\vec{r},t)$ and $\delta T_t(\vec{r},t)$. The space-dependent deviation $\delta T_s(\vec{r},t)$ varies from zero to $\delta T(\vec{r},\infty)$ during the transient. In the present study, $\delta T(\vec{r},\infty)$ is also the maximum $\delta T_s(\vec{r},t)$. The maximum for $\delta T_t(\vec{r},t)$ is obtained by examining the difference between $T_d(\vec{r},t)$ and $T_e(\vec{r},t)$ plots. Here $T_d(\vec{r},t)$ is calculated directly using

$$T_d(\vec{r},t) = 1 + \frac{[T_c(\vec{r},t) - 1][T_e(\vec{r},\infty) - 1]}{T_c(\vec{r},\infty) - 1} \qquad (6)$$

which is derived from Equations 2b and 4. The relative magnitudes of $\delta T_s(\vec{r},t)$ and $\delta T_t(\vec{r},t)$ indicate whether the functional deviations $\delta T(\vec{r},t)$ are primarily space- or time-dependent.

## C. Asymptotic Time Region

Fluxes in the asymptotic region increase with a constant period. Direct comparison of experimental and TRIMHX fluxes were made well beyond the prompt jump. Also, because the asymptotic period is related to the insertion worth calculated

by static TRIMHX, experimental and TRIMHX worths are readily compared. The experimental worth is obtained with an Inhour period analysis of the flux measurements.[2,3]

## III. SPACE-TIME EXPERIMENT

Static measurements were made for a sequence of five reactor loadings culminating in the experimental loading given in Figure 1. These measurements provide data for adjusting cross section parameters for use in the TRIMHX calculations. The measurements and loadings are analogous to those reported in the earlier experiments[2,3] and are outlined in Table I.

The transient experiment was performed similarly to the previous ones.[2,3] Briefly, the reactor was made critical with the $^{235}U$ perturbation rod removed from the core (see Figure 1). Then the $^{235}U$ rod was magnetically released into the core and fell to a rest position governed by a snubbing device. During the rod drop, a *Visicorder*[7] noted the rod release time (magnet current interruption) and recorded the times when the rod bottom (defined by a small magnet) passed induction coils positioned near the top and bottom of the core. Beginning three seconds before the rod drop, the neutron flux monitored by each $^{10}B$-lined detector[8] was measured with a picoammeter,[9] a voltage-to-frequency converter,[10] and a minicomputer[11] operated in a multiscaling mode. During multiscaling, the channel dwell times were 0.1 sec for the first 6.0 sec, 1 sec for the next 60 sec,

and 10 sec for the remainder of the transient. Resulting measurements for fluxes and tilts are given in Figures 2 and 3, respectively.

## IV. TRIMHX ANALYSIS

### A. Space-Model Development

The reactor was modeled with a 2-dimensional (hex-z) representation since the core was axially uniform. Axial bucklings were obtained from critical water height measurements and core extrapolation distances as determined by gold pin activations. Cross sections for the 2-dimensional calculations were obtained with an integral transport code, GLASS[12], and then adjusted to yield static TRIMHX agreement with measurements of axial bucklings and flux profiles. All TRIMHX calculations utilized two energy groups and a coarse mesh approximation[13] with one mesh point per cell. Convergence criteria were $\pm 10^{-6}$ in $k_{eff}$ and $\pm 5 \times 10^{-5}$ in flux.

In developing the cross section parameters, each transport calculation region was composed of one control rod assembly surrounded by six fuel assemblies, except for regions of the reflector and tank wall which had uniform properties. The infinite lattice GLASS calculations for the seven-assembly cluster yielded cross sections for the hexagonal cells associated with each assembly and determined supercell average cross sections for the cluster. Supercell average cross sections were used for all clusters except those containing detector or perburbation

sites. Experimental measurements at these sites were best modeled with cell detail. The GLASS cross sections were adjusted prior to the TRIMHX calculation as follows:

1) $\Sigma_c$ of each control cell was adjusted so that an infinite lattice diffusion calculation for its seven-cell cluster yielded the GLASS buckling of the supercell.
2) $\nu\Sigma_f$ of each cell and supercell was adjusted so that TRIMHX calculations for each static experiment agreed with measurements for buckling and flux profiles.
3) $\Sigma_c$ of each detector site cell was adjusted for the worth of detectors.

A detailed summary of these cross section adjustments is given in Table A.1 of the appendix.

B. Time-Model Development

Time-dependent modeling used with TRIMHX is given below:

1) Delayed neutron group structure for this fuel as given in Reference 2.
2) Linear change from unperturbed cross sections to perturbed cross sections during the measured $^{235}U$ rod insertion interval of 0.48 sec.
3) Time steps: 0.025 sec for $0 \leq t \leq 0.6$ sec
   0.05 sec for 0.6 sec $\leq t \leq$ 1.0 sec
   0.1 sec for 1.0 sec $\leq t \leq$ 13 sec

TRIMHX does not permit changes in the inverse velocities (from GLASS), but changes due to the perturbation were insignificant. The perturbed inverse velocities were used for the calculation.

## V. RESULTS

Experimental and calculated results are given in Table II and Figures 2 and 3. Comparisons based on these results are presented for the DNH and asymptotic time regions. All deviations are expressed as % of corresponding measured values.

The overall agreement for fluxes in the DNH time region is exemplified in Figure 2, where TRIMHX and measured fluxes agree to within 3.0%. Deviations between TRIMHX and experimental tilts are compared in Table II. The maximum space-dependent deviation $\delta T_s(\vec{r},t)_{max}$ is 2.5%. The $\delta T_t(\vec{r},t)$ values were obtained using the graphs in Figure 3, yielding a maximum value of 0.3%.

The approach of the fluxes and tilts toward the asymptotic region is predicted well by TRIMHX, as indicated in Figures 2 and 3. For the asymptotic region, a 2.4% disagreement exists between static TRIMHX worth calculations and Inhour measurements of the insertion worth.

The space-dependent and time-dependent deviations [$\delta T_s(\vec{r},t)$ and $\delta T_t(\vec{r},t)$] between experimental and TRIMHX tilts are quite small. In the present study, $\delta T_s(\vec{r},t)$ is more than five times larger than $\delta T_t(\vec{r},t)$, suggesting that improved cross section modeling could eliminate the bulk of the discrepancy $\delta T(\vec{r},t)$. An effort to reduce the discrepancy demonstrated that $\delta T_s(\vec{r},t)$ is more sensitive to cross section adjustment than $\delta T_t(\vec{r},t)$. These results indicate that the time-model parameters are well-chosen in this study. Furthermore, similar analyses indicate that

this time modeling was appropriate in the earlier experiments,[2,3] and that the small deviations $\delta T(\vec{r},t)$ probably could be removed by more elaborate cross section adjustments.

## VI. CONCLUSIONS

The experimental tilts and fluxes in the present and earlier[2,3] studies agree well with TRIMHX calculations that utilize the adjusted cross sections. Thus, the TRIMHX time-dependence has been tested and demonstrated to be accurate for a variety of reactor coupling strengths. For a tilt $T(\vec{r},t)$ a measure of DNH is given by

$$m\ (DNH) = \frac{T(\vec{r},\infty) - T(\vec{r},t_d)}{T(\vec{r},\infty) - 1} = 1 - f(\vec{r},t_d) \qquad (7)$$

where $t_d$ is the time just after the prompt jump in tilt is completed. (In the present experiment, $t_d$ was 0.5 sec).

Values of m(DNH) for the various experiments are given in Table III. Each experiment involved transients caused by fuel inserted in core locations similar to that of the present experiment. Detector locations $\vec{r}$ were also similar. Agreement between experimental and calculated m(DNH) is $\sim\pm 0.01$ for each case.

The m(DNH) measurements of Table III are given for reactors with various flux shapes and core radii. These features determine the lattice coupling strength. It is observed that m(DNH) increases as coupling strength decreases. Using this framework, Table III indicates a broad range of experiments for which TRIMHX

has been successfully tested. Thus, for space-time diffusion calculations, these results provide comprehensive confirmation for W. B. Stacey's premise that "a calculational model capable of predicting certain static characteristics of an assembly will be successful in predicting the outcome of transients carried out in that assembly if delayed neutrons are treated properly".[5]

## ACKNOWLEDGMENTS

The authors wish to express their thanks to P. B. Parks for his assistance and advice throughout all phases of the study. Helpful discussions with C. E. Ahlfeld, W. E. Graves, F. J. McCrosson, R. J. Pryor, and J. D. Spencer are also gratefully acknowledged.

References & Footnotes

[1]M. R. BUCKNER and J. W. STEWART, *Nucl. Sci. Eng.*, *59* 289 (1976).

[2]P. B. PARKS, N. P. BAUMANN, R. L. CURRIE, and C. E. JEWELL, *Nucl. Sci. Eng.*, *59*, 298 (1976).

[3]W. G. WINN, P. B. PARKS, N. P. BAUMANN, and C. E. JEWELL, *Nucl. Sci. Eng.*, *65*, 254 (1978).

[4]A. E. DUNKLEE, *The Heavy Water System of the Process Development Pile*, USAEC Report DP-567, E. I. du Pont de Nemours and Company, Aiken, SC (1961).

[5]W. M. STACEY, JR., *React. Technol.*, *14*, 169 (1971).

[6]In the asymptotic region ($t \to \infty$), the flux $\Phi(\vec{r},t)$ and delayed precursors $C_i(\vec{r},t)$ are factorable as $\phi(\vec{r})e^{\alpha t}$ and $C_i(\vec{r})e^{\alpha t}$, respectively. Consequently, the space-time diffusion equations can be reduced to a static diffusion equation with eigenvalue $k_{eff}$. The $\phi(\vec{r})$ calculated from these equations will depend directly on the cross sections which are coefficients of $\phi(\vec{r})$. The tilt, given in Equation 1, will depend only on $\phi(\vec{r})$ for detectors A and B, because the $e^{\alpha t}$ factors cancel. Thus, $T(\infty)$ depends directly on $\phi(\vec{r})$ which, in turn, depends directly on the cross section adjustments.

[7]Honeywell, Denver, Colorado, Model 1508 *Visicorder*.

[8]Reuter Stokes Electronic Components, Inc., Cleveland, Ohio, Model RSN-229A.

[9]Keithley Instruments, Inc., Cleveland, Ohio, Models 409 and 417. Brookhaven Instrument Corp., Austin, Texas, Model 10002.

[10]*Wavetek*, San Diego, California, Model 120-021 Function Generator.

[11]Tracor Northern Inc., Middleton, Wisconsin, Model TN-11.

[12]The GLASS code (Generalized Lattice Analysis Subsystem) includes the RAHAB code referred to in References 3 and 4. For more detail, refer to H. C. Honeck, *The JOSHUA System*, USERDA Report DP-1380, E. I. du Pont de Nemours and Company, Savannah River Laboratory, Aiken, SC (1975) and H. C. Honeck, *Trans. Amer. Nucl. Soc.*, *14*, 224 (1971).

[13]H. L. Dodds, Jr., H. C. Honeck, and D. E. Hostetler, *Trans. Amer. Nucl. Soc.*, *21*, 223 (1975).

## APPENDIX

The cross section adjustments for the basic TRIMHX analysis are presented in Table A.I. The GLASS values needed to be adjusted only a few percent to obtain GRIMHX agreement with static measurements. Similar adjustments for the alternative analyses were also small.

Complete cross section data are available from the authors for use in testing alternative space-time codes. These data include the GLASS-generated cross section parameters, axial buckling measurements, and gold pin flux measurements.

TABLE I

Static Measurements

| Loading Sequence[a] | Description[b] | Measurements[c] |
|---|---|---|
| 1. Base lattice | 60°-symmetry; fuel and control assemblies in Rings 1 and 2; heavy water throughout reflector. | CWH, Au |
| 2. Detector Sites | Heavy water removed from inner thimbles of 18 fuel assemblies; 6 voided aluminum thimbles placed in reflector. | CWH |
| 3. Perturbation Sites | Two voided aluminum thimbles replaced fuel assemblies to accommodate perturbation insertion. | CWH, Au |
| 4. Detectors | Ten $^{10}B$-lined detectors placed in selected voided thimbles. | CWH |
| 5. Perturbation | $^{235}U$ perturbation rod inserted into a perturbation site thimble. | CWH |

---

[a] Case n corresponds to base lattice with modifications accumulated in Case 2 through Case n.

[b] Refer to Figure 1.

[c] CWH - critical water height measured for axial buckling; Au - gold pin activations for flux profile.

TABLE II

Percent Deviations of TRIMHX from Experimental Measurements

| Tilt* | $\delta T_s(\vec{r},t)_{max}$ | $\delta T_t(\vec{r},t)_{max}$ |
|---|---|---|
| S1/N1 | -2.1 | 0.0 |
| S2/N2 | -2.5 | -0.1 |
| S3/N3 | -1.7 | 0.3 |
| S4/N4 | -0.5 | -0.1 |

TABLE III

Delayed Neutron Holdback

| Radial Flux | Core Radius[a] | Lattice Coupling | m(DNH)[b] | Reference |
|---|---|---|---|---|
| peaked | large | strong | 0.19 | Experiment 1 of Ref. 1 |
| flat | large | moderate | 0.24 | Experiment 2 of Ref. 2[c] |
| dished | large | weak | 0.35 | Experiment 2 of Ref. 1 |
| dished | small | strong | 0.18-core<br>0.15-reflector | Present work |

[a]Radii: small = present experiment (Figure 1)

large = small + 1-1/2 rings of fuel clusters

[b]Measured values are given; corresponding TRIMHX calculations of m(DNH) agreed to within $\pm$0.01 of measured values.

[c]An asymmetric perturbation was applied in this experiment; the tilt included in the table is radial-azimuthal, as it was for all the other cases.

TABLE A.I

Cross Section Adjustment for Basic Analysis

| | Experimental Sequence[a] | Region Normalized[b] | Variation from GLASS[c] Ring | Ring | Reflector |
|---|---|---|---|---|---|
| 1. | Normalize base lattice ($B_z^2 = 83.369 \times 10^{-6}$ cm$^{-2}$) | all supercells | X1.0000 +0.8323% | X1.0000 +0.3306% | X1.0000 - |
| 2. | Install detector assemblies without detectors ($B_z^2 = 85.383 \times 10^{-6}$ cm$^{-2}$) | detector site supercells | X0.999147 +0.5462% | X0.978885 +0.0459% | X1.0000 - |
| 3. | Install perturbation sites without $^{235}U$ slugs ($B_z^2 = 86.132 \times 10^{-6}$ cm$^{-2}$) | perturbation site supercells | | X0.92644 -0.3468% | |
| 4. | Install detectors ($B_z^2 = 84.596 \times 10^{-6}$ cm$^{-2}$) | detector site cells | $\Delta\Sigma_{c_1}$ | $\Delta\Sigma_{c_1}$ | $2\Delta\Sigma_{c_1}$ |
| | | | $\Delta\Sigma_{c_2}$ | $\Delta\Sigma_{c_2}$ | $2\Delta\Sigma_{c_2}$ |
| | | | ($\Delta\Sigma_{c_1} = 0.01544 \times 10^{-4}$ cm$^{-1}$) | | |
| | | | ($\Delta\Sigma_{c_2} = 0.05940 \times 10^{-3}$ cm$^{-1}$) | | |
| 5. | Insert $^{235}U$ into perturbation site ($B_z^2 = 89.385 \times 10^{-6}$ cm$^{-2}$) | perturbation site cell | | X N.A. +3.4044% | |

[a] $B_z^2 = [\pi/(CWH + TED)]^2$; where the critical water height (CWH) was measured from tank bottom, and the total extrapolation distance (TED = 47.6 ± 0.5 cm) was measured with vertically spaced gold pins. The absolute error of each $B_z^2$ is ± 0.25 x $10^{-6}$ cm$^{-2}$ and due principally to the error in TED. However, the relative error in comparing differences between the $B_z^2$ is only ± 0.010 x $10^{-6}$ cm$^{-2}$, as it is due principally to the error in CWH of ± 0.02 cm.

[b] The base lattice calculations used supercell average fewgroup parameters. These averages were successively replaced with appropriate cell parameters at the special sites denoted in Figure 1.

[c] Multiplicative (X) factors for $\Sigma_c$ of septifoil, % adjustments for $\nu\Sigma_f$ and $\Delta\Sigma_c$ and for detector addition.

LIST OF FIGURE TITLES

FIGURE 1. Face map of lattice assemblies spaced 17.78 cm center-to-center

FIGURE 2. Measured flux response compared with TRIMHX results

FIGURE 3. Calculated tilts ($T_d$ and $T_c$) compared to measured tilts ($T_e$). These curves yield $\delta T_s = T_c - T_d$ and $\delta T_t = T_d - T_e$. (Note that tilts begin at 3.5 sec, which defines "t = 0.")

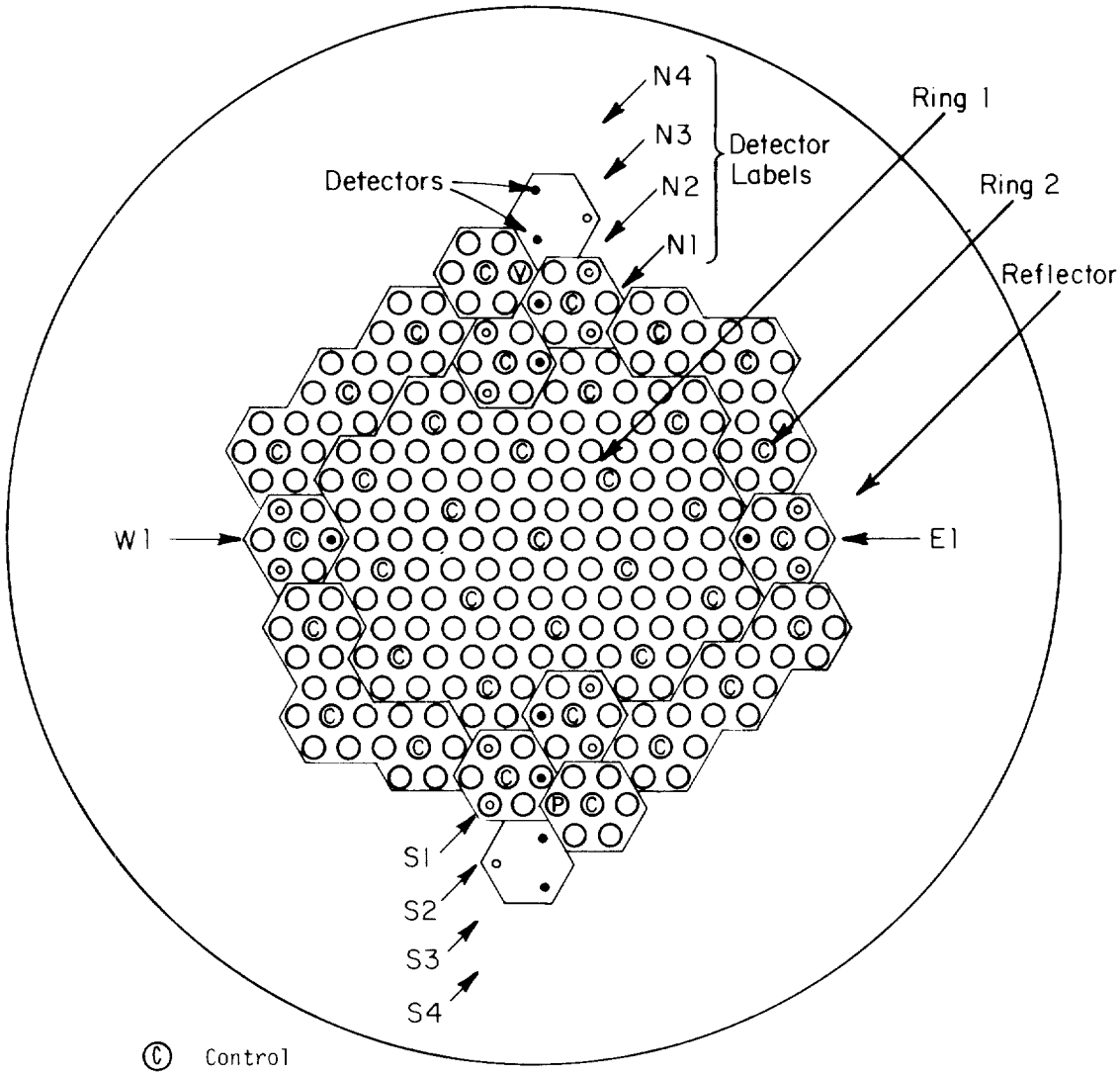


FIG. 1. Face map of lattice assemblies spaced 17.78 cm center-to-center

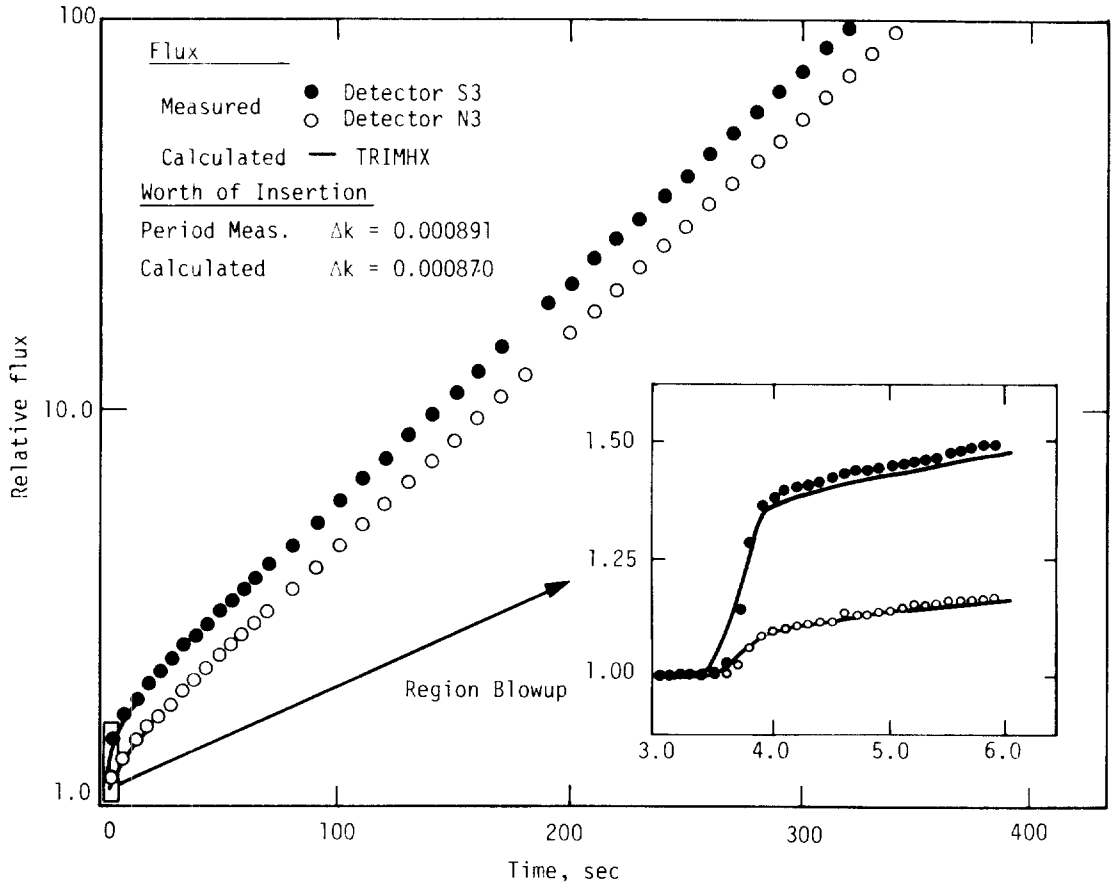


FIG. 2. Measured flux response compared with TRIMHX results

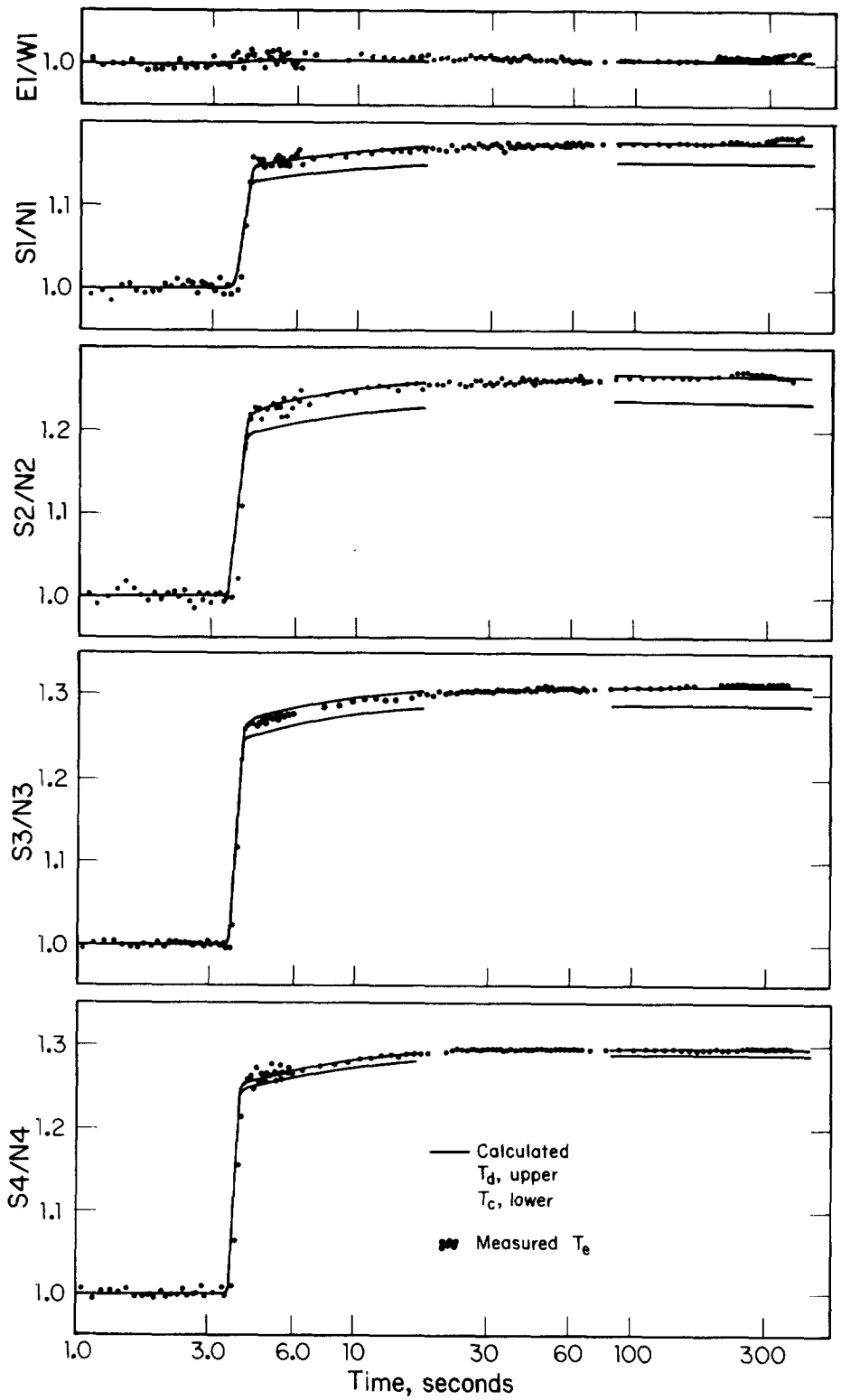


FIG. 3. Calculated tilts ($T_d$ and $T_c$) compared to measured tilts ($T_e$). These curves yield $\delta T_s = T_c - T_d$ and $\delta T_t = T_d - T_e$. (Note that tilts begin at 3.5 sec, which defines "t = 0.")